Chemical Physics 143 (1990) 163–170
North-Holland

MULTI-ELECTRODE DIELECTRIC SPECTROSCOPY

M.W. EVANS [1]

Department of Chemistry, Bourne Laboratory, Royal Holloway and Bedford New College, University of London, Egham, Surrey TW20 0EW, UK

Received 23 August 1989; in final form 29 December 1989

The technique of multi-electrode dielectric spectroscopy is introduced to describe the molecular cross correlation dynamics of dipolar ensembles. The symmetry of the electrodes in the laboratory frame (X, Y, Z) is described with point group theory and is imparted to the ensemble dynamics in terms of new cross correlation functions in frame (X, Y, Z). By comparing the dielectric loss and permittivity for different electrode symmetries, the effect on the spectrum of cross correlation functions can be isolated. A number of practically feasible electrode arrangements is suggested for the frequency range Hz to MHz.

1. Introduction

Conventional dielectric spectroscopy [1–5] utilises an electrode symmetry that can be described in terms of an appropriate point group symmetry [6–8], $C_{\infty v}$. This is the same point group symmetry as that of a dipolar linear molecule, and is made of one positive and one negative electrode, causing a dipolar molecular ensemble to become polarised with a frequency dependent dielectric loss and permittivity [1–5]. The polarisation produces information on the time correlation function of the net permanent molecular dipole moment, conventionally through linear response theory and the fluctuation–dissipation theorem [9–13]. This correlation function is essentially the Fourier transform of the dielectric loss divided by angular frequency [14]. The electrode technique in dielectric spectroscopy suffices from about Hz to MHz, just below the microwave. At higher frequencies waveguides are required.

In this paper a potentially new and useful technique is introduced which utilises electrode symmetries other than the simple $C_{\infty v}$ in the laboratory frame (X, Y, Z). Each electrode arrangement has its own point group symmetry in frame (X, Y, Z). The purpose of the new technique is to induce the existence in (X, Y, Z) of new time cross correlation functions (ccfs) of the molecular ensemble dynamics. By comparing the frequency dependence of dielectric loss and permittivity from different electrode symmetries, the effect of the underlying ccfs can be isolated. This provides much more information, in principle, that that available from the conventional $C_{\infty v}$ electrode arrangement alone. Wherever the conventional dielectric approach is used, the multi-electrode approach is also valid, allowing considerably scope for development in several disciplines [1–5].

2. The link between electrode symmetry and ccfs

The new technique rests on a straightforward application of the third principle of group theoretical statistical mechanics (gtsm) [15–22], which implies that the complete symmetry of an external force field (in this case an electric field) is imparted to ensemble averages to which the field is applied. The complete symmetry includes parity inversion ($\hat{P}$), time reversal ($\hat{T}$), and all irreducible representations in the appropriate point group. For field free achiral ensembles at thermodynamic equilibrium this is $R_h(3)$, the point group of all possible rotations and reflections [15]. An applied field lowers $R_h(3)$ symmetry, so that ensemble averages which vanished in $R_h(3)$ become visible in the new point group in the field-

[1] Present address: Theory Center, Cornell University, Ithaca, NY 14850, USA.

0301-0104/90/$ 03.50 © Elsevier Science Publishers B.V. (North-Holland)

applied steady state, or in the transient condition directly after the field is applied. In conventional dielectric spectroscopy there is one positively charged electrode opposite a negatively charged counterpart. The appropriate point group established in frame (X, Y, Z) by this arrangement is $C_{\infty v}$.

Having established the point group, $C_{\infty v}$, we apply the second principle [15,16] of gtsm, which states [15–17] that an ensemble average exists in that point group if the former's irreducible representation contains the totally symmetry irreducible representation (tsr) at least once. In the absence of an electric field between our two electrodes, there is no polarisation of the sample, i.e. the ensemble average $\langle \boldsymbol{\mu} \rangle$ vanishes, where $\boldsymbol{\mu}$ is the molecular permanent dipole moment. When the field is switched on, this average exists in (X, Y, Z) and the sample is polarised. In the absence of the field, the ensemble point group is $R_h(3)$, and the irreducible representation of $\langle \boldsymbol{\mu} \rangle$ in $R_h(3)$ is that of $\boldsymbol{\mu}$ itself (first principle of gtsm, the Neumann–Curie principle [19]). This is denoted $D_u^{(1)}$, which does not contain the tsr $D_g^{(0)}$. The ensemble average $\langle \boldsymbol{\mu} \rangle$ vanishes in $R_h(3)$. In the presence of the field, the ensemble point group is $C_{\infty v}$, and the irreducible representation of $\langle \boldsymbol{\mu} \rangle$ in $C_{\infty v}$ is $\Sigma^+ + \Pi$, using the literature [6–8] character table. This contains the tsr, Σ^+, once, signifying that $\langle \mu_Z \rangle$ exists in the Z axis of frame (X, Y, Z), the axis of polarisation.

As soon as $C_{\infty v}$ is established as the relevant point group in (X, Y, Z), principle three allows *any* ensemble average that includes the tsr, not just the polarisation, $\langle \mu_Z \rangle$. An interesting example is the ccf $\langle v(t)\omega(0) \rangle$ between the linear and angular velocities of a diffusing molecule of the ensemble. The existence of two components of this ccf under electric polarisation was first realised in the mid eighties, using computer simulation [23–26]. It is not described in conventional dielectric relaxation theory [1–5]. The irreducible representation of this nine-element tensor in $C_{\infty v}$ is

$$\Gamma(v)\Gamma(\omega) = (\Sigma^+ + \Pi)(\Sigma^- + \Pi) , \qquad (1)$$

wherein the tsr appears from the direct product [6–8] $\Pi\Pi$ signifying the existence of

$$\langle v_X(t)\omega_Y(0) \rangle = -\langle v_Y(t)\omega_Z(0) \rangle . \qquad (2)$$

These elements have equal and opposite time dependence, and this is exactly what was found [23–26] by computer simulation. Note that the details of the time dependence itself are governed by fundamental equations of motion in the molecular ensemble. The other seven elements vanish by symmetry.

The question naturally arises of how to isolate the equal and opposite elements experimentally, how, at least, to discern their effect on the measurable dipole autocorrelation function. Multi-electrode dielectric spectroscopy approaches this fundamental problem through the use of point groups different from $C_{\infty v}$, constructed from different electrode arrangements in frame (X, Y, Z). Each electrode arrangement imparts its point group symmetry to ensemble averages through principle three.

3. Examples of electrode point groups and their ensemble averages

We consider three electrode point groups of decreasing symmetry in (X, Y, Z): C_{2v}, C_{1h} and C_1. The electrode geometries appropriate to these point groups are illustrated in fig. 1; geometries which are modelled on molecular structures satisfying the same point group symmetries. The water molecule has C_{2v} point group symmetry, and the electrode arrangement for C_{2v} is appropriately modelled as the triangular arrangement in fig. 1A, consisting of one positively charged electrode (a), and two negatively and equally charged electrodes (b) and (c). The three electrodes are wired up to separate emf sources ("batteries") so that the charge on each can be varied independently of the two others. This allows the total potential between the three electrodes to be adjusted to be the same as that across the conventional $C_{\infty v}$ two-electrode arrangement, in order to normalise inductance and capacitance. Having calibrated the two cells ($C_{\infty v}$ and C_{2v}) we are in a position to compare directly the *frequency dependence* of the dielectric loss and permittivity. The underlying effect of cross correlation functions shows up as differences in these frequency dependencies for the same net potential in Z.

A slightly more complicated C_{2v} arrangement is shown in fig. 1B, modelled after a C_{2v} molecule such as dichloromethane. This has five electrodes, arranged in three dimensions and independently

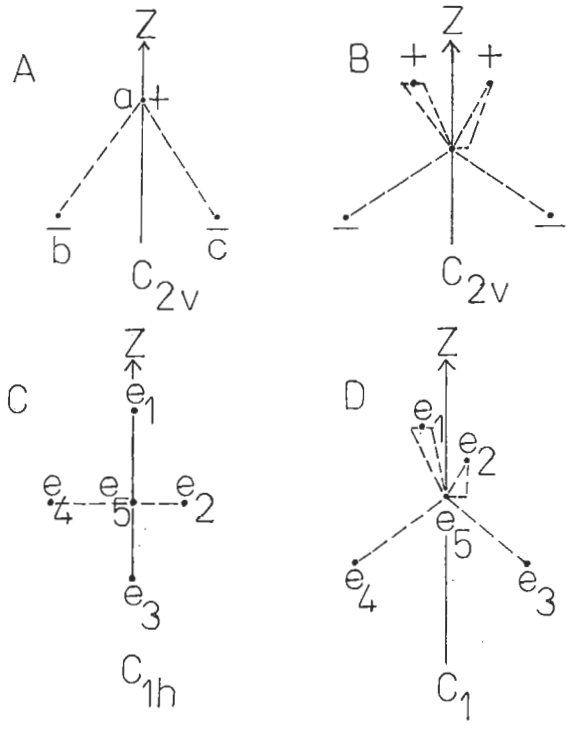

Fig. 1. Point electrode arrangements of given point group symmetry. (A) Planar C_{2v} symmetry, (a) is positively charged and (b) and (c) are independently negatively charged with separate circuits. The charge on (b) is the same as that on (c). The distance ab=ac. (B) Three-dimensional C_{2v} symmetry, modelled after a tetrahedral molecule such as dichloromethane. The off-centre positive charges are equal, and so are the off-centre negative charges. The central charge can be either positive or negative. The two distances positive–central and negative–central must be equal. The separate distances positive–central and negative–central can be unequal. (C) Planar C_{1h} symmetry. This symmetry is maintained by arbitrary dissymetric planar arrangements of charge, illustrated by e_1 to e_5. A simpler C_{1h} arrangement is as in (A) with charge (b) not equal to charge (c). (D) Enantiomeric C_1 symmetry. This is tetrahedral, as in (B), but with charges all different.

charged as shown. This three-dimensional arrangement allows cross correlation functions to develop satisfactorily between variables in the X and Y axes. The net polarization is measured in the Z axis, as shown.

3.1. Cross correlation functions from C_{2v} symmetry electrodes

The irreducible representation of the ccf $\langle v(t)\omega(0)\rangle$ in C_{2v} is the direct product

$$\Gamma(v)\Gamma(\omega)=(A_1+B_1+B_2)(A_2+B_1+B_2)\,, \qquad (2)$$

which contains the tsr twice. Principle two implies the existence of two *independent* elements from the products

$$B_1B_1: \quad \langle v_X(t)\omega_Y(0)\rangle\,, \qquad (3)$$

and

$$B_2B_2: \quad \langle v_Y(t)\omega_X(0)\rangle\,. \qquad (4)$$

The molecular dynamics of a dipolar molecular ensemble under a C_{2v} electrode arrangement are therefore fundamentally different from those under a $C_{\infty v}$ arrangement. This difference is due to the influence of time cross correlation functions, of which $\langle v(t)\omega(0)\rangle$ is an example; an influence which can be observed as a difference in the dielectric loss and permittivity spectra of the two cells, thus isolating the effect of the ccfs for any given sample.

3.2. Cross correlations from C_{1h} symmetry electrodes

The C_{1h} arrangement of electrodes is illustrated in fig. 1C, where there are four unequal charges in a plane. The net polarisation is measured in the Z axis as illustrated. The irreducible representation of the ccf $\langle v(t)\omega(0)\rangle$ in C_{1h} is given by

$$\Gamma(v)\Gamma(\omega)=(2A'+A'')(A'+2A'')\,, \qquad (5)$$

wherein the tsr, A′, occurs four times. There are four independent elements of the ccf in frame (X, Y, Z) compared with two for C_{2v} and one for $C_{\infty v}$. The four elements for C_{1h} are from:

$$2A'A': \quad \langle v_Z(t)\omega_X(0)\rangle$$

and

$$\langle v_Y(t)\omega_X(0)\rangle\,, \qquad (6)$$

$$2A''A'': \quad \langle v_X(t)\omega_Z(0)\rangle$$

and

$$\langle v_X(t)\omega_Y(0)\rangle \qquad (7)$$

and if the C_{1h} cell is calibrated against the C_{2v} and $C_{\infty v}$ cells, we expect to see differences in the frequency dependences of the dielectric loss and permittivity due to the presence of more nonvanishing elements of ccfs such as $\langle v(t)\omega(0)\rangle$.

3.3. Cross correlations from the C_1 symmetry electrode arrangement

The C_1 electrode arrangement is shown in fig. 1D, modelled on a chiral pentatomic molecule such as (R)-bromochlorofluoromethane. All five charges are different. In calibrating this cell, the net potential in the Z axis is adjusted to be the same as that across the two electrodes of the $C_{\infty v}$ cell and the same as in the Z axes of the other cells. For this purpose the five electrodes are wired to independent batteries in order to be able to charge up independently.

The irreducible representation of $\langle v(t)\omega(0)\rangle$ in C_1 is the product

$$\Gamma(v)\Gamma(\omega) = 3A\,3A = 9A\,, \qquad (8)$$

which contains the tsr, A, nine times. In this case all nine elements of the ccf exist in frame (X, Y, Z). If we construct the mirror image cell from fig. 1D all nine elements of the ccf change sign. It is possible therefore to measure directly the effect of this change of sign on the frequency dependent dielectric loss and permittivity by comparing results from mirror image cells, calibrated to the same net potential in Z.

4. Discussion

The principles of group theoretical statistical mechanics imply that different electrode symmetries measure fundamentally different ensemble molecular dynamics, due to time cross correlation functions. This has been illustrated with respect to one member of the set of non-vanishing time ccfs generated by each electrode arrangement in the laboratory frame. Electrode point group symmetries have been used which generate respectively one, two, four and nine independent elements of this ccf, $\langle v(t)\omega(0)\rangle$, directly in frame (X, Y, Z). The presence of these elements changes fundamentally the nature of the molecular dynamics of the dipolar ensemble under measurement, and this change works its way through into measurable differences in the frequency dependences of the dielectric loss and permittivity for each electrode point group symmetry.

In order to implement this method practically, circuits are needed which allow the proper calibration of each cell, so that the net potential in one axis (Z) is the same for each cell. This appears to require the capability for independent charging of each electrode in order to adjust the potential.

The method is quite generally applicable and, in principle, reveals details of time cross correlations which are otherwise not available. In dielectric spectroscopy, these cross correlations are *always* present, in the simplest $C_{\infty v}$ cell, there is one element of $\langle v(t)\omega(0)\rangle$ which was discovered by computer simulation [23–26]. With other electrode arrangements there are more elements, whose influence can be detected by comparing directly results from calibrated cells.

5. Computer simulation

A computer simulation with $C_{\infty v}$ and C_{1h} electrode symmetries was carried out using a sample of 108 water molecules interacting with a site–site potential fully described in the literature [21–30]. The effect of $C_{\infty v}$ electrode symmetry was simulated with an electric field in the X axis of the laboratory frame (X, Y, Z), whose effect was mimicked with a torque in the forces loop of the algorithm as described in the literature [30]. The C_{1h} electrode symmetry was mimicked with two electric fields on unequal field strength in the X and Z axes of (X, Y, Z). To test the third principle of gtsm the symmetry effect at a molecular level was computed through time correlation functions, using an integration time step of 5.0 fs with segments of up to 6000 time steps. Correlation functions were evaluated with running time averaging. Fields of sufficient strength to show the presence of symmetry dependent correlation functions were used in the simulations. They were energetically equivalent to approximately 25 kJ per mole.

The autocorrelation function (acf) of the permanent molecular dipole moment is essentially the Fourier transform of the frequency dependent complex dielectric permittivity [1–4], and the rotational velocity acf, that of the the time derivative of the dipole moment, is essentially the Fourier transform of far infrared power absorption and frequency dependent refractive index [9]. It was found that both types of correlation function and spectra depend markedly on the electrode symmetry. A direct comparison for the rotational velocity acf is provided in fig. 2. This

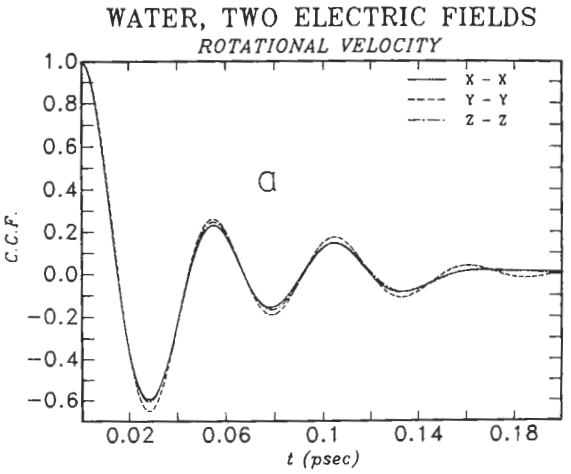

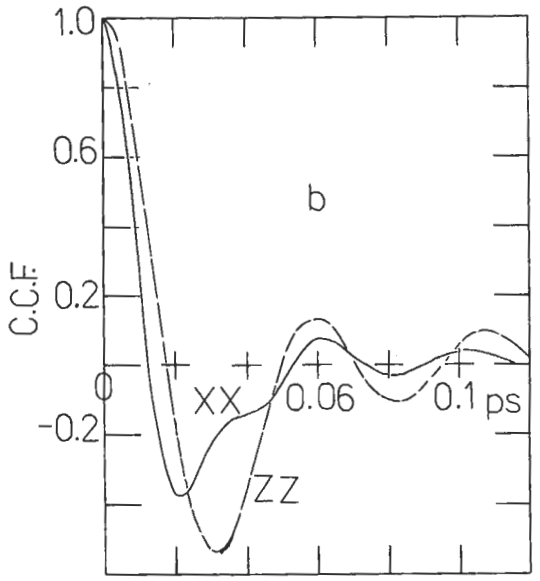

Fig. 2. (a) C_{1h} symmetry of electrodes, the three diagonal components of the rotational velocity autocorrelation function in frame (X, Y, Z) of the laboratory. Computer simulation of liquid water at 293 K, 1 bar. (b) As for (a), XX and ZZ elements with $C_{\infty v}$ electrode symmetry.

confirms our earlier argument that electrode symmetry affects the dielectric spectrum from static to THz (far infrared) frequencies.

The specific symmetry effects of the $C_{\infty v}$ and C_{1h} electrode arrangements on molecular dynamics at a local level can be illustrated with the use of particular time cross correlation functions (ccfs). The C_{1h} symmetry is expected from principle three to support

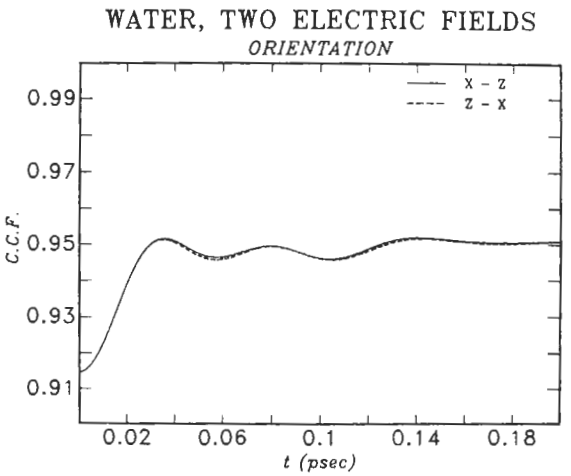

Fig. 3. Off-diagonal XZ and ZX elements of the permanent dipole moment correlation function with C_{1h} electrode symmetry. The corresponding elements for $C_{\infty v}$ electrode symmetry vanish.

more of these in the ensemble of water molecules, and this is bourne out by the following illustrations. Fig. 3 shows the symmetry allowed (X, Z) and (Z, X) elements of the orientational ccf produced by C_{1h} symmetry, and this was confirmed in the simulation, where they vanish in the "statistical noise". The same pattern of results was obtained (fig. 4) for the (X, Z) and (Z, X) elements of rotational velocity, angular velocity (fig. 5), and linear center of mass velocity (fig. 6). In all these cases the corresponding elements

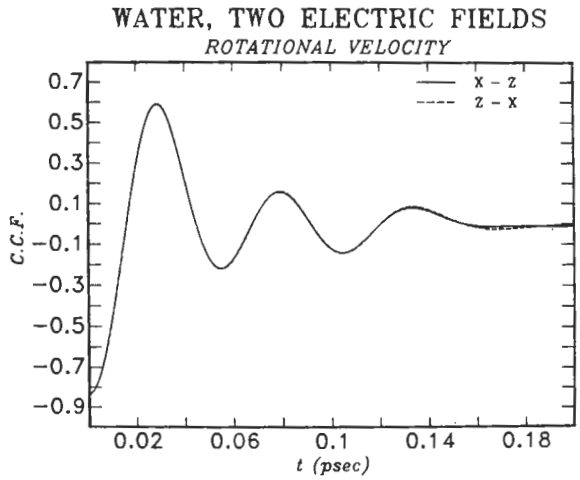

Fig. 4. As for fig. 3, rotational velocity correlation function.

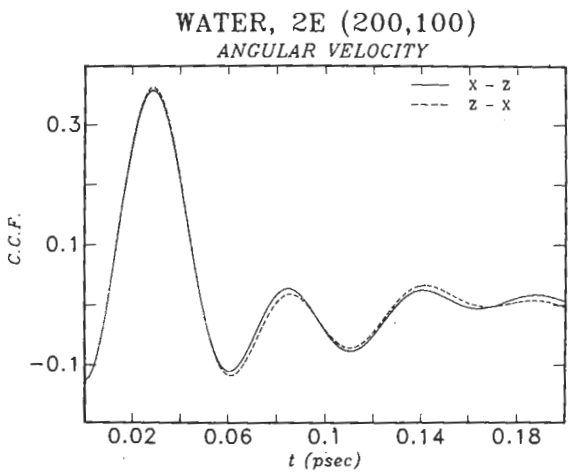

Fig. 5. As for fig. 3, angular velocity correlation function.

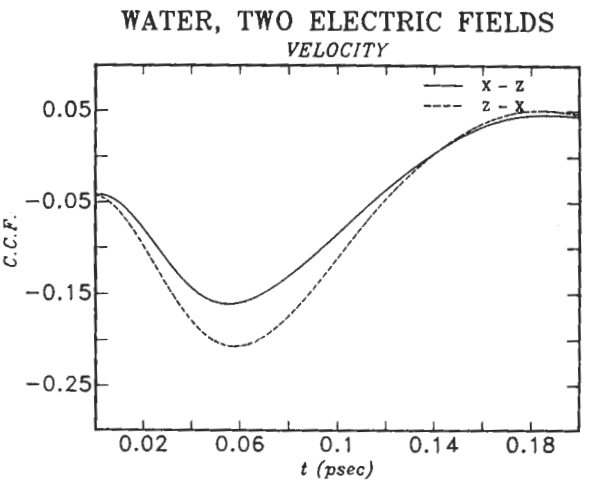

Fig. 6. As for fig. 3, center of mass linear translational velocity correlation function.

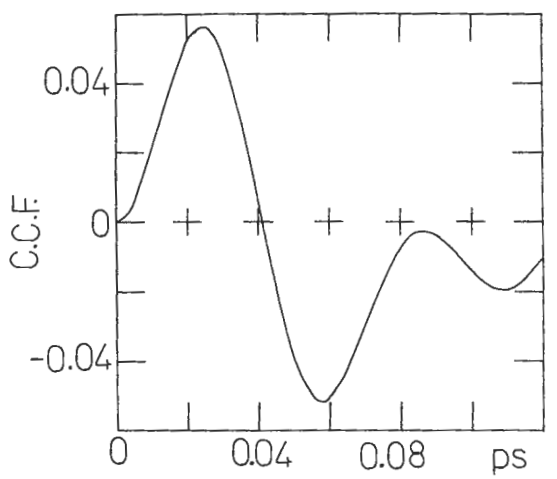

Fig. 7. The YZ element of the cross correlation function between linear and angular velocity, using $C_{\infty v}$ electrode symmetry. This is the negative of the ZY element by symmetry.

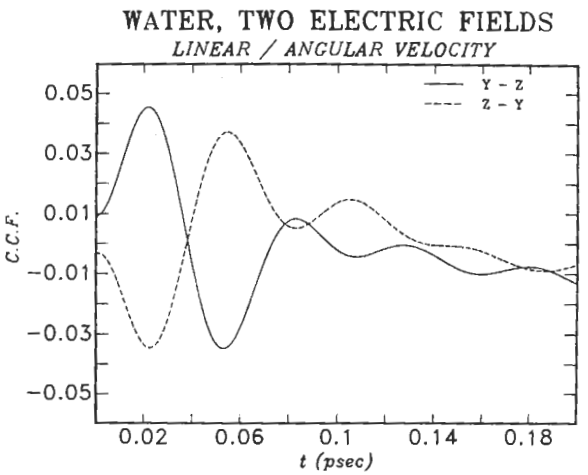

Fig. 8. The YZ and ZY elements of the ccf of fig. 7, C_{1h} electrode symmetry.

with $C_{\infty v}$ electrode symmetry vanished in the background noise of the computer simulation in accordance with principle three of gtsm. The corresponding effect on the effective far infrared spectrum is clear (fig. (2)). Each of these ccfs was computed with 6000 time step segments.

A particularly interesting example of the change of electrode symmetry appears in the time cross correlation function between molecular linear center of mass velocity and the same molecule's angular velocity [23–26]. With $C_{\infty v}$ electrode symmetry there is only one independent element (fig. 7), as predicted by principle three [15–20]. For an X axis electric field this is

$$\langle v_Z(t)\omega_Y(0)\rangle = -\langle v_Y(t)\omega_Z(0)\rangle \ .$$

With C_{1h} symmetry electrode placement there are clearly four elements of this ccf, which are shown in figs. 8 and 9, two each for the X and Z axis unequal electric fields making up the (planar) C_{1h} electrode symmetry. The ccfs are

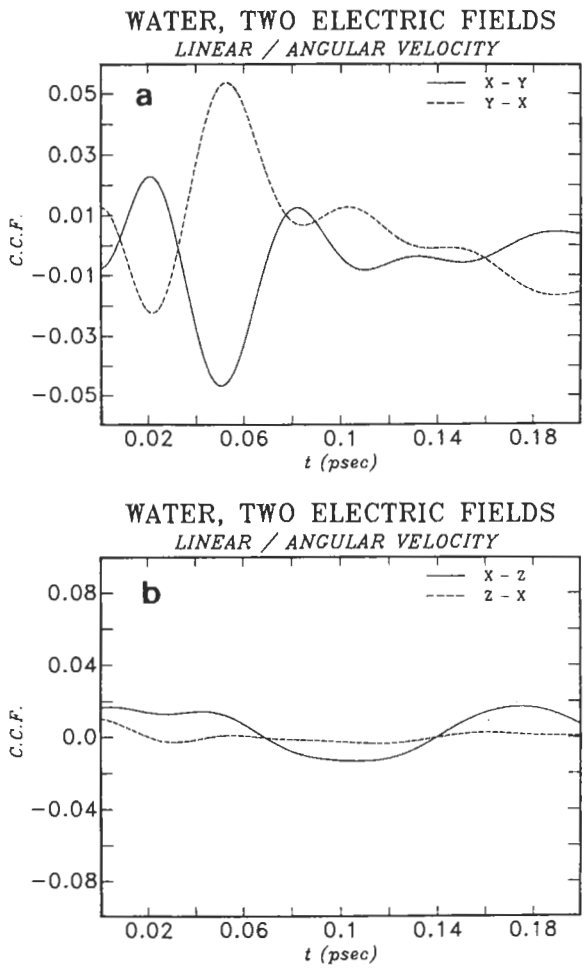

Fig. 9. (a) As for fig. 8, the XY and YX elements. (b) As for fig. (8), illustrating the fact that the XZ and ZX elements vanish in the noise, confirming gtsm for C_{1h} electrode symmetry, which allows four off-diagonal elements only (see text).

$\langle v_X(t)\omega_Y(o)\rangle$, $\langle v_Y(t)\omega_X(0)\rangle$

and

$\langle v_Z(t)\omega_Y(0)\rangle$, $\langle v_Y(t)\omega_Z(0)\rangle$.

The corresponding change in observable spectral behaviour in the frequency dependent complex permittivity can be observed experimentally using four electrodes arranged in a plane, generating unequal electric field strengths at right angles. This spectrum can be matched by computer simulation and the latter used to produce abundant molecular dynamical detail. This is a promising method for the investigation of a wide range of materials [1–4] by multi-electrode dielectric spectroscopy. There is no practical difficulty in implementing a variety of electrode symmetries for the same sample of dielectric, be this solid, liquid or liquid crystalline.

Acknowledgement

The Academic Board of Royal Holloway and Bedford New College is thanked for the award of a Research Fellowship; and the EEC for financial support. Part of this research was conducted using the resources of the Center for Theory and Simulations in Science and Engineering (Cornell Theory Center), which receives major funding from the National Science Foundation and IBM corporation, with additional support from New York State and the Corporate Research Institute.

References

[1] N.E. Hill, A.H. Price, W.E. Vaughan and M. Davies, Dielectric Properties and Molecular Behaviour (Van Nostrand–Reinhold, New York, 1969).
[2] C.P. Smyth, Dielectric Behavior and Structure (McGraw-Hill, New York, 1965).
[3] P. Bordewijk and C.J.F. Bottcher, Theory of Electric Polarisation, Vols. 1, 2 (Elsevier, Amsterdam, 1973, 1979).
[4] M. Davies (Senior Reporter), Dielectric and Related Molecular Processs, Vols. 1–3 (Chem. Soc., London, 1972–1977).
[5] National Research Council (USA), Digest of Literature on Dielectrics (National Academy of Sciences, Washington).
[6] R.L. Flurry Jr., Symmetry Groups, Theory and Chemical Applications (Prentice–Hall, Englewood Cliffs, 1980).
[7] F.A. Cotton, Chemical Applications of Group Theory (Wiley–Interscience, New York, 1963).
[8] D.S. Urch, Orbitals and Symmetry (Penguin Books, Harmondsworth, 1970).
[9] M.W. Evans, G.J. Evans, W.T. Coffey and P. Grigolini, Molecular Dynamics (Wiley–Interscience , New York, 1982).
[10] D.A. McQuarrie, Statistical Mechanics (Harper and Row, New York, 1975).
[11] R. Balescu, Equilibrium and Non-Equilibrium Statistical Mechanics (Wiley, New York, 1975).
[12] M.W. Evans, I. Prigogine and S.A. Rice, eds., Advances in Chemical Physics, Vol. 63 (Wiley–Interscience, New York, 1989).

[13] P. Resibois and M. de Leener, Classical Kinetic Theory of Fluids (Wiley–Interscience, New York, 1977).
[14] C. Brot, in: Dielectric and Related Molecular Processes, Vol. 2 (Chem. Soc., London) p. 1.
[15] M.W. Evans, Chem. Phys. Letters 152 (1988) 33; 158 (1989) 375.
[16] M.W. Evans, Chem. Phys. 127 (1988) 413; 132 (1989) 1; 135 (1989) 187.
[17] M.W. Evans, Phys. Letters A 134 (1989) 409.
[18] M.W. Evans, Mol. Phys. 67 (1989) 1195.
[19] M.W. Evans, Phys. Rev. A 39 (1989) 6041.
[20] M.W. Evans and D.M. Heyes, Mol. Phys. 65 (1988) 1441; in press.
[21] M.W. Evans and D.M. Heyes, Mol. Sim., in press.
[22] M.W. Evans and D.M. Heyes, Proceedings of the 1989 NATO/CECAM Workshop on Simulation of Complex Flows (Brussels), in press.
[23] M.W. Evans, Phys. Letters A 102 (1984) 248.
[24] M.W. Evans, Phys. Rev. A 31 (1985) 3947.
[25] M.W. Evans, Physica Scripta 31 (1985) 419.
[26] M.W. Evans, Physica B, C 131 (1985) 273.
[27] M.W. Evans, G.C. Lie and E. Clementi, J. Chem. Phys. 88 (1988) 5157.
[28] M.W. Evans, G.C. Lie and E. Clementi, Phys. Letters A 130 (1988) 289.
[29] M.W. Evans, G.C. Lie and E. Clementi, J. Mol. Liq. 40 (1989) 89.
[30] M.W. Evans, G.C. Lie and E. Clementi, Phys. Rev. A 37 (1988) 2551.